JOURNAL OF SOLID STATE CHEMISTRY 17, 363–372 (1976)

Structures of a Semiconducting and a Metallic Phase in the Fe_yZrSe_2 System

A. GLEIZES,* J. REVELLI, AND JAMES A. IBERS

Departments of Chemistry and Material Science and the Materials Research Center, Northwestern University, Evanston, Illinois 60201

Received August 28, 1975; in revised form October 28, 1975

Studies of the Fe_yZrSe_2 system have led to a semiconducting phase for $y = 0.16$ and to a metallic phase for $y = 0.41$. The structures of both phases have been established through single-crystal X-ray measurements. The compound $Fe_{0.16}ZrSe_{1.94}$ crystallizes with one formula unit in space group D_{3d}^3–$P\bar{3}m1$ of the trigonal system in a cell of dimensions $a = 3.763\,(1)$, $c = 6.118\,(1)$ Å. The structure is of the CdI_2–NiAs intermediate type with octahedral coordination of Se atoms about both the Fe and Zr atoms. The compound $Fe_{0.41}ZrSe_2$, the metallic phase, crystallizes with six formula units in space group D_6^6–$P6_322$ of the hexagonal system in a cell of dimensions $a = 6.011\,(1)$, $c = 12.787\,(1)$ Å. The structure is the same as that of MNb_3S_6 (M = Mn, Fe, Co, Ni). In this structure, the Fe atoms are in octahedral holes while the Zr atoms are trigonal prismatically coordinated by Se atoms.

Introduction

Numerous recent studies of the intercalation properties of the layered metal dichalcogenides have led to a variety of new quasi-binary systems of the form M_yTX_2 where T is a transition metal of group IVB, VB, or VIB; X is S, Se, or Te; and M can be either an alkali metal, a transition metal, or a post-transition metal. In general, it is found that the basic structure of the TX_2 host material remains unchanged as the intercalate atoms go into the van der Waals' gap between the layers. On the other hand, the electronic and magnetic properties of the intercalation complex may be dramatically different from the host material.

For example, in group IVB dichalcogenides one finds the CdI_2 structure as the basic structure and octahedral coordination for the transition metal. Upon intercalation, the coordination of the IVB transition metal remains octahedral and the excess metal atoms occupy either octahedral, tetrahedral, or trigonal prismatical holes between layers. Trichet and Rouxel have studied the system M_yZrS_2 (M = Fe, Co, Ni) (*1*, *2*) where M atoms occupy tetrahedral holes of the CdI_2-type structure. However, in the A_yZrS_2 system (A = Li, Na, K, Rb) studied by Trichet, Cousseau, and Rouxel (*2–4*) the insertion of alkali metal gives rise to several structures derived from the CdI_2 type, in which the coordination of the alkali metal can be either octahedral, trigonal prismatic, or both, the zirconium coordination remaining octahedral. Until the present study, in all group IVB transition metal dichalcogenides and their intercalate derivatives the IVB transition metal has exhibited octahedral coordination.

Although there are several polytypes in group VB dichalcogenides, the low-temperature modification exists with a trigonal prismatic coordination of the transition metal. Unlike the group IVB dichalcogenides, those of group VB are normally metallic. The change in the transition metal coordination in going from group IVB (octahedron) to group VB (trigonal prism) has been related to the change

* On leave from Laboratoire de Chimie de Coordination du C.N.R.S. Université Paul Sabatier, Toulouse, France.

in metal–chalcogen bonding character from ionic to more covalent (*5*). The change in bonding character is partly responsible for the change in electrical behavior. Compounds of the form M_yNbS_2 and M_yTaS_2 (M = Mn, Fe, Co, Ni) have been investigated by van den Berg and Cossee (*6*). For $0 \leqslant y \leqslant \frac{1}{3}$, the extra metal atoms occupy octahedral holes of the 2H-NbS_2-type structure; for $y = \frac{1}{3}$, a superstructure $a' = \sqrt{3}a$ appears with no other change in metal coordination. The systems remain metallic upon intercalation and all are antiferromagnetic except Mn_yNbS_2 and Mn_yTaS_2, which are ferromagnetic. Compounds M_yNbSe_2 (M = Ti, V, Cr, Mn, Fe, Co, Ni) (*7*, *8*), on the other hand, were found to exist in the limits $0 \leqslant y \leqslant \frac{1}{2}$ with two distinct types of superlattices at compositions $y = \frac{1}{4}$ ($a' = 2a$) and $y = \frac{1}{3}$ ($a' = a\sqrt{3}$).

These experimental results led us to consider the system Fe_yZrSe_2, which had not been previously examined. Like ZrS_2, $ZrSe_2$ crystallizes in the CdI_2-type structure (*9*) and is a semiconductor (*10*). Owing to the somewhat smaller band gap of $ZrSe_2$ as compared with ZrS_2 (*11*), the iron atom would be more likely to donate electrons to the conduction band of $ZrSe_2$. Thus, for some critical iron concentration one might expect the system to undergo a semiconductor–metal transition.

Indeed such a transition was observed, accompanied by a discontinuous change in structure. A semiconducting phase, with $E_g \geqslant 0.2$ eV determined from electrical resistivity measurements, was found to exist for $0 < y < 0.23$,[1] and a metallic phase was observed for the composition $Fe_{0.41}ZrSe_2$ (*13*). Here, we report on the single-crystal structures of the metallic compound and the semiconducting compound ($y = 0.16$).

Synthesis and Chemical Analysis: Experimental

Appropriate quantities of the elements, Fe (99.5%, 325 mesh, Alfa Organics/Inorganics), Zr (99.9%, 80 mesh, Alfa Organics/Inorganics), and Se (99.9999%, pellet, Gallard Schlesinger Corp.) were weighed out and placed in quartz ampoules 20 × 1.7 cm. These ampoules were evacuated to $\approx 10^{-3}$ Torr followed by the addition of about 120 Torr partial pressure of hydrogen chloride gas as a transport agent (*14*). The tubes were then sealed and placed in tubular furnaces. After 5 or 6 days at 450°C, the reactions were found to be complete yielding fine, free flowing, homogeneous powders. After 2 weeks in a temperature gradient of 965–870°C for the metallic phase and 935–840°C for the semiconducting phase, the samples were slowly cooled (about 40°C/hr) and removed from the ovens.

No transport occurred for the metallic composition; rather, large crystals (~1 cm^2 in cross section) formed at the hot end of the ampoule. These crystals are thin hexagonal plates and are silver metallic in luster. They are brittle and resist attack by hot concentrated nitric acid. The semiconducting material also tended to form hexagonal plates nearer to the hot end of the ampoule. However, these crystals are metallic green in luster, resembling $ZrSe_2$ crystals. They are much less stable to air than even $ZrSe_2$; a blue tarnish will form on the surface after about 1 or 2 weeks of exposure to air. Furthermore, upon grinding, the crystals exhibit a "greasy" texture and react vigorously with dilute nitric acid.

The metallic-type sample had a composition $Fe_{0.465\pm0.015}Zr$–$Se_{2.00\pm0.05}$ (Schwarzkopf Analytical Laboratories; see Table I). It should be noted that we were successful in obtaining this particular phase in only one sample batch. We believe that the difficulty in

TABLE I

METALLIC Fe_yZrSe_2 ANALYSES[a]

	Se (%)	Zr (%)	Fe (%)
	57.39	32.15	9.39
	56.49	33.44	9.25
	57.00		
Average	56.96	32.80	9.32

[a] Formula: $Se/Zr = 2.00 \pm 0.05$; $Fe/Zr = 0.464 \pm 0.015$.

[1] This homogeneity range is very similar to that found by Ahouandjinou and Trichet (*12*).

preparing this phase is a result of a very narrow homogeneity range of composition and a complicated mechanism of formation.

Single-phase semiconducting material was obtained when the initial Fe/Zr ratio was less than 0.23 ± 0.05. Analysis of the sample from which a single crystal was drawn for structure investigation was carried out by means of X-ray fluorescence. Crystals were exposed to nitric acid, and after evaporation of the solution, the remaining powder was pressed into a pellet. Pellets of standard composition were obtained in the same way by treating mixtures of zirconia, iron, and selenium with nitric acid. The $K\alpha_1$ peaks of the three elements were counted during 10- or 20-sec intervals at their intensity maxima, with X-ray voltage of 40 kV and current of 20 mA. Comparison of measured intensities of unknown and standards led to the formula $Fe_{0.23\pm0.05}ZrSe_{1.94\pm0.06}$ for the sample.

Collection of X-ray Data

(*1*) *Semiconducting* $Fe_{0.16}ZrSe_{1.94}$

Preliminary precession photographs showed $\bar{3}m$ Laue symmetry and no systematic absences. Unit-cell constants from these photographs were near those of $ZrSe_2$.

A single crystal was mounted for data collection on a Picker FACS-I computer controlled four-circle X-ray diffractometer equipped with a scintillation counter and a pulse height analyzer. The crystal was a thin, regularly shaped hexagonal platelet. The indices of its eight faces were of the forms {001} and {100}. As measured by a traveling microscope eyepiece, the crystal was 0.13 mm thick with a mean diameter across the hexagonal base of 0.24 mm and a calculated volume of 0.40×10^{-3} mm^3.

The unit-cell constants, determined from a least-squares refinement (*15*) of the setting angles of 13 reflections, are $a = 3.763$ (1) Å and $c = 6.118$ (1) Å at 21°C. These values are slightly smaller than those found in nonstoichiometric $ZrSe_2$ prepared at 800°C: $3.772 > a > 3.768$ and $6.128 < c < 6.150$ Å when Se/Zr decreases from 1.965 to 1.850 (*16*, *17*). The density of the sample was measured pycnometrically in toluene and found to be 5.61 (4) g/cm^3; this value is consistent with that of 5.7 (2) g/cm^3 calculated for one formula unit per cell.

As molybdenum radiation was not available at the time this compound was studied, intensity data were collected using Cu radiation, ($CuK\alpha_1 = 1.540562$ Å) prefiltered through 1 mil of Ni foil. Reflections were scanned in the θ–2θ mode from 1.5° below the $K\alpha_1$ peak to 1.5° above the $K\alpha_2$ peak. The 2θ-scan speed was 2°/min and the background was counted for 10 sec at the two extremes of the scan. The take-off angle was 2.7°. The counter positioned 30 cm from the crystal was preceded by an aperture of 6.0×5.5 mm. The pulse height analyzer was set to admit 90% of the Cu$K\alpha$ peak and copper foil attenuators were automatically inserted if the intensity exceeded about 7000 cps during the scan. Six standard reflections collected every 100 reflections showed no significant change. A total of 421 reflections in the range $5° < 2\theta < 121°$ was scanned. These data were processed (*15*) using a p of 0.04 in the estimation of standard deviations. The data were then corrected for absorption using a μ of 688 cm^{-1} calculated for $Fe_{0.3}ZrSe_2$; the transmission factors ranged from 0.026 to 0.352 (*18*). Next, reflections that would be equivalent for various point groups were averaged (*19*). The best agreement was obtained for $\bar{3}m1$ and so space group D_{3d}^3–$P\bar{3}m1$ was used in the structure refinement.

(*2*) *Metallic* $Fe_{0.41}ZrSe_2$

Preliminary precession photographs indicated Laue symmetry $6/mmm$ and systematic absences $00l$ with l odd, consistent with space group D_6^6–$P6_322$.

A single crystal was mounted on the diffractometer for intensity data collection. This crystal was a pentagonal-based rectangular prism with seven very regular faces of indices $\bar{1}20$, $\bar{2}10$, $\bar{1}\bar{1}0$, $1\bar{2}0$, 100, 001, $00\bar{1}$. The crystal was 0.124 mm in height with mean basal diameter of 0.16 mm and a calculated volume of 0.18×10^{-2} mm^3.

The unit-cell constants derived from a least-squares refinement of the setting angles of 16 reflections are $a = 6.011$ (1) Å and

$c = 12.787$ (1) Å (Mo$K\alpha_1$ radiation, $\lambda = 0.70930$ Å, $t = 21°C$). Combined with the density measured in toluene of 6.77 (3) g/cm^3 and the mass corresponding to $Fe_{0.465(15)}ZrSe_{2.00(5)}$ ($M = 275$ (5)), the lattice constants lead to $Z = 5.93$ (13), that is to six formula units in a cell.

The intensities were collected by the θ–2θ scan technique, using Mo$K\alpha$ radiation monochromatized by the (002) face of an oriented graphite crystal. A take-off angle of 2.0° was found suitable and the counter aperture was set to 4.0 × 5.5 mm. The 2θ-scan speed was 2°/min. The background was counted at 0.9° below the $K\alpha_1$ peak and at 0.9° above the $K\alpha_2$ peak for 10 or 20 sec, depending on whether 2θ was less or greater than 90°, respectively. Reflections with positive indices and $h \geq k$ were collected in the range $6° < 2\theta < 125°$, and reflections with all three negative indices and $|h| \geq |k|$ were collected in the range $6° < 2\theta < 75°$. The intensities of six standard reflections collected every 100 reflections showed no significant variations.

Among the 1883 independent reflections thus collected 573 had $F_o^2 > 3\sigma(F_o^2)$ and were used in subsequent calculations. Of these, 382 had $h, k, l \geq 0$.

The data were corrected for absorption, using a μ of 332 cm^{-1} for the composition $Fe_{0.5}ZrSe_2$. The transmission factor ranged from 0.032 to 0.163.

Structure Refinement

Refinement of each structure was effected by full-matrix least-squares techniques. Throughout the refinement, the function minimized was $\sum w(|F_o| - |F_c|)^2$ where $|F_o|$ and $|F_c|$ are the observed and calculated structure amplitudes and the weight w is $4F_o^2/\sigma^2(F_o^2)$. The agreement indices R and R_w are defined as $R = \sum(||F_o| - |F_c||)/\sum F_o$ and $R_w = (\sum(|F_o| - |F_c|)^2/\sum wF_o^2)^{1/2}$. The atomic scattering factors and anomalous terms for Zr, Se, and Fe are from the tabulation in (*20*).

(*1*) *Semiconducting* $Fe_{0.16}ZrSe_{1.94}$

The Patterson map showed three strong peaks which could be interpreted by placing he Zr atom on the origin site and Se atoms in sites $2d \pm (\frac{1}{3}, \frac{2}{3}, z \approx \frac{3}{4})$. Initial refinement of this z coordinate and the scale factor led to an R index of 0.105. A subsequent difference Fourier map showed as its only significant feature a peak at $(0, 0, \frac{1}{2})$ which we attribute to Fe. An ensuing refinement, which included an isotropic description of thermal motion and secondary extinction, led to an R of 0.064. Attempts to improve the R index by placing the Fe in tetrahedral sites, as occurs in Fe_yZrS_2 (1, 2), were not successful.

The formula deduced from the refined values of the Se and Fe occupancy factors was $Fe_{0.16}ZrSe_{1.94}$, in satisfactory agreement with that of $Fe_{0.23\pm0.05}ZrSe_{1.94\pm0.06}$ from X-ray fluorescence analysis. Based on the composition derived from the structure analysis a new absorption correction ($\mu = 617$ cm^{-1}) was applied to the data. Subsequent refinement led to final values of R and R_w of 0.059 and 0.063 for the 60 observations and 8 variables. The error in the observation of unit weight was 3.03 electrons. Analysis of $\sum w(|F_o| - |F_c|)^2$ as a function of $|F_o|$, setting angles, and Miller indices revealed no unusual trends. On a final difference Fourier map the maximum electron density was 1.7 e/Å^3.

Values of observed and calculated structure amplitudes are given in Table IIa. Refined atomic parameters are reported in Table III. Interatomic distances compared with the equivalent one of $ZrSe_2$ (16) are tabulated in Table IV.

(*2*) *Metallic* $Fe_{0.41}ZrSe_2$

From the Patterson map, Se atoms had to be in 12*i* positions, either $(\frac{1}{3}, 0, \frac{1}{8})$ or $(\frac{2}{3}, 0, \frac{1}{8})$, and Zr atoms in either $2b \pm (0, 0, \frac{1}{4})$, $2c \pm (\frac{1}{3}, \frac{2}{3}, \frac{1}{4})$, $2d \pm (\frac{1}{3}, \frac{2}{3}, \frac{3}{4})$, or $2a$ $(0, 0, 0; 0, 0, \frac{1}{2})$ and $4f \pm (\frac{1}{3}, \frac{2}{3}, z \approx 0$ and $\frac{1}{2})$ positions.

Initial refinements were carried out using only those reflections having positive indices. Among the combinations of Zr and Se positions possible from the Patterson map, a significantly lower agreement index was obtained for Zr in $4f$ and $2a$ and Se in $12i$ with $x \approx \frac{2}{3}, y \approx 0, z \approx \frac{1}{8}$. An ensuing difference Fourier map showed as its only significant features peaks in the $2b$, $2c$, and $2d$ positions. The next cycle of least-squares refinement included an isotropic model for thermal

TABLE II

TABLE IIa: OBSERVED AND CALCULATED STRUCTURE AMPLITUDES FOR THE SEMICONDUCTING $Fe_{0.[illegible]}ZrSe_{1.94}$

K	L	FO	FC	K	L	FO	FC	K	L	FO	FC	K	L	FO	FC	K	L	FO	FC	K	L	FO	FC	K	L	FO	FC
***** H = 0 *****				***** H = 1 *****				0	-2	48	57	-3	4	2	2	-1	4	54	52	***** H = 3 *****				0	-1	15	15
								0	2	47	49	-2	-5	5	5	0	-5	43	41					0	0	50	48
0	0	0	107	-3	4	7	8	0	4	10	10	-2	-3	47	45	0	-4	8	9	-4	-1	7	7	0	1	16	15
0	1	25	27	-1	-6	19	22	0	5	53	47	-2	-1	14	13	0	-3	15	14	-1	-3	39	39	0	2	12	11
0	2	21	21	-1	-3	18	18	1	5	8	9	-2	0	5	4	0	-2	41	38	-1	-2	37	37	0	3	14	14
0	3	31	30	-1	-1	55	73	2	-3	12	12	-2	1	59	56	0	2	47	45	-1	-1	12	11	0	4	37	33
0	4	71	62	-1	0	6	6					-1	-6	8	8	0	4	2	3	-1	0	4	4	1	0	3	3
0	5	10	9	-1	1	18	18	***** H = 2 *****				-1	-3	26	25	1	2	34	32	-1	1	48	47				
0	6	10	10	-1	3	53	55					-1	-2	17	16	2	2	9	9	0	-4	37	38	***** H = 4 *****			
				0	-6	35	36	-4	0	42	41	-1	0	67	71					0	-3	19	19				
				0	-4	3	3	-4	1	13	13	-1	1	22	20					0	-2	12	11	-3	1	34	35

TABLE IIb: OBSERVED AND CALCULATED STRUCTURE AMPLITUDES FOR THE METALLIC $Fe_{0.[illegible]}ZrSe_{[illegible]}$

H	L	FO	FC	H	L	FO	FC	H	L	FO	FC	H	L	FO	FC	H	L	FO	FC	H	L	FO	FC	H	L	FO	FC
***** K = -5 *****				-6	-1	19	20	-7	-8	37	28	-1	-11	158	159	0	-16	272	225	5	1	28	30	1	18	90	90
				-5	-15	78	75	-7	-7	78	75	-1	-10	125	122	0	-14	150	150	5	9	26	29	1	19	91	93
-5	-5	41	43	-5	-14	28	29	-7	-6	44	44	-1	-9	92	93	0	-12	51	54	6	0	277	266	1	20	113	112
-5	-4	110	110	-5	-13	26	31	-7	-5	57	54	-1	-8	49	45	0	-10	74	19	6	2	67	61	1	23	48	47
-5	-3	59	59	-5	-12	126	128	-7	-4	140	136	-1	-7	191	189	0	-8	424	426	6	4	47	47	1	24	34	31
-5	-2	50	50	-5	-11	88	88	-7	-3	75	75	-1	-6	89	80	0	-6	178	174	6	6	99	95	1	26	54	54
-5	-1	55	53	-5	-10	77	77	-7	-2	62	61	-1	-5	148	144	0	-4	105	107	6	8	229	223	1	27	47	49
-5	0	22	26	-5	-9	52	50	-7	-1	68	67	-1	-4	372	353	0	-2	131	123	6	14	93	95	1	28	55	56
				-5	-8	31	31	-7	0	22	28	-1	-3	218	210	0	0	0	691	6	16	140	143	1	31	32	35
***** K = -4 *****				-5	-7	95	97	-5	-9	21	19	-1	-2	144	136	0	2	130	123	6	22	67	70	2	1	28	27
				-5	-6	51	52	-5	-6	18	15	-1	-1	182	197	0	4	101	107	6	24	74	78	2	3	20	22
-5	-2	20	16	-5	-5	70	71	-5	-1	20	20	-1	0	69	62	0	6	174	174	7	3	19	20	2	5	23	23
-4	-13	29	27	-5	-4	172	172	-4	-18	72	73					0	8	395	426	7	5	24	24	2	6	13	12
-4	-12	113	115	-5	-3	98	98	-4	-16	29	33	***** K = 0 *****				0	10	22	19	8	0	19	16	2	7	19	19
-4	-11	78	78	-5	-2	75	74	-4	-15	93	95					0	12	51	54	8	9	24	23	2	9	20	22
-4	-10	66	70	-5	-1	89	89	-4	-14	31	33	-8	-9	22	23	0	14	147	150	8	25	16	14	2	13	19	16
-4	-9	43	44	-5	0	30	31	-4	-13	39	39	-6	-16	141	143	0	16	217	225	9	0	149	148	3	3	25	26
-4	-8	29	30	-4	-13	24	17	-4	-12	161	160	-6	-14	92	95	0	22	99	103	9	2	39	39	3	5	26	20
-4	-7	83	85	-4	-6	18	17	-4	-11	112	116	-6	-12	27	24	0	24	105	109	9	6	57	57	3	11	17	14
-4	-6	48	48	-4	-2	19	19	-4	-10	93	95	-6	-8	223	223	0	30	58	61	9	8	132	130	3	13	23	23
-4	-5	61	62	-3	-9	24	27	-4	-9	64	66	-6	-6	97	95	1	1	25	28	9	14	60	58	4	0	38	35
-4	-4	153	152	-3	-7	19	20	-4	-8	36	34	-6	-4	45	47	1	3	31	32	9	16	93	91	4	1	121	122
-4	-3	86	85	-3	-1	26	29	-4	-7	129	131	-6	-2	63	61	1	4	12	5	9	22	48	47	4	2	95	92
-4	-2	65	67	-2	-20	100	102	-4	-6	62	61	-6	0	285	266	1	5	35	34	11	9	21	18	4	3	139	135
-4	-1	76	77	-2	-19	84	82	-4	-5	94	97	-5	-9	25	29	1	7	19	17	12	0	81	82	4	4	236	228
-4	0	28	29	-2	-18	79	81	-4	-4	226	228	-5	-1	27	30	1	9	19	20	12	2	20	21	4	5	93	97
				-2	-17	20	22	-4	-3	134	135	-4	-5	33	32	1	11	19	14	12	4	17	10	4	6	42	61
***** K = -3 *****				-2	-16	35	35	-4	-2	96	92	-4	-3	30	27	1	13	24	22	12	6	32	31	4	7	126	131
				-2	-15	106	108	-4	-1	121	122	-3	-16	196	198	2	1	35	37	12	8	74	74	4	8	33	34
-6	-8	160	159	-2	-14	39	35	-4	0	39	35	-3	-14	130	132	2	3	14	17					4	9	63	66
-6	-6	69	70	-2	-13	45	45	-3	-5	28	29	-3	-12	45	44	2	5	19	18	***** K = 1 *****				4	10	93	95
-6	-4	28	27	-2	-12	181	182	-3	-3	23	27	-3	-10	23	20	2	7	23	23					4	11	113	116
-6	-2	47	47	-2	-11	133	135	-2	-17	20	16	-3	-8	361	347	2	9	30	30	1	0	71	62	4	12	156	160
-6	0	187	183	-2	-10	108	107	-2	-13	18	16	-3	-6	145	140	3	0	478	453	1	1	174	197	4	13	38	39
-5	-9	27	24	-2	-9	77	78	-2	-9	21	23	-3	-4	80	83	3	2	95	88	1	2	143	136	4	14	31	33
-5	-1	22	24	-2	-8	41	37	-2	-7	18	18	-3	-2	94	88	3	4	76	83	1	3	208	210	4	15	93	95
-4	-5	26	25	-2	-7	156	156	-2	-6	15	12	-3	0	447	453	3	6	142	140	1	4	348	353	4	16	34	33
-4	-3	19	21	-2	-6	71	68	-2	-5	22	23	-2	-17	21	20	3	8	340	347	1	5	145	144	4	18	72	73
-3	-16	158	158	-2	-5	112	115	-2	-3	22	22	-2	-9	31	30	3	10	20	20	1	6	89	80	4	19	72	74
-3	-14	104	105	-2	-4	271	274	-2	-2	18	14	-2	-7	24	23	3	12	43	44	1	7	188	189	4	20	91	93
-3	-12	27	29	-2	-3	157	162	-2	-1	29	28	-2	-5	15	18	3	14	129	132	1	8	51	45	4	23	59	56
-3	-8	253	255	-2	-2	108	107	-1	-20	111	112	-2	-3	20	17	3	16	196	198	1	9	93	93	4	24	25	26
-3	-6	106	107	-2	-1	146	148	-1	-19	94	93	-2	-1	33	37	3	18	24	11	1	10	124	122	4	26	49	46
-3	-4	56	58	-2	0	48	44	-1	-18	89	90	-1	-13	25	22	3	22	91	93	1	11	155	159	4	27	44	42
-3	-2	67	67					-1	-17	21	25	-1	-11	16	14	3	24	97	99	1	12	205	210	4	28	45	49
-3	0	319	308	***** K = -1 *****				-1	-16	37	37	-1	-9	20	20	3	30	52	57	1	13	53	53	5	2	18	17
								-1	-15	124	124	-1	-7	17	17	4	3	31	27	1	14	35	36	6	3	19	19
***** K = -2 *****				-7	-11	71	70	-1	-14	37	36	-1	-5	36	34	4	5	27	32	1	15	122	124	6	5	25	22
				-7	-10	63	63	-1	-13	52	53	-1	-3	33	32	4	11	17	14	1	16	37	37	6	6	21	14
-7	-6	19	15	-7	-9	38	39	-1	-12	209	210	-1	-1	26	28	4	13	21	25	1	17	27	25	7	0	27	28

H	L	FO	FC	H	L	FO	FC	H	L	FO	FC	H	L	FO	FC	H	L	FO	FC	H	L	FO	FC
7	1	67	67	2	12	179	182	8	8	72	24	9	2	29	28	10	1	23	24	***** K = 7 *****			
7	2	61	61	2	13	45	45	8	9	28	28	9	4	22	13	10	2	21	23				
7	3	74	75	2	14	32	35	8	10	51	47	9	6	41	40	10	3	29	27	7	0	21	16
7	4	138	136	2	15	107	108	8	11	49	51	9	8	91	92	10	4	51	53	7	1	24	26
7	5	53	54	2	16	33	35	8	12	80	79	9	14	45	42	10	5	22	20	7	2	25	25
7	6	42	44	2	18	79	81	8	13	22	18	9	16	68	68	10	7	27	28	7	3	34	29
7	7	77	75	2	19	81	82	8	14	23	19					10	9	21	15	7	4	53	57
7	8	32	28	2	20	101	102	8	15	49	46	***** K = 4 *****								7	5	22	21
7	9	40	39	2	23	60	61	8	18	40	39					***** K = 5 *****				7	6	19	18
7	10	63	63	2	24	24	28	8	19	43	39	4	0	30	29					7	7	32	30
7	11	73	70	2	26	46	50	8	20	54	53	4	1	76	77	5	0	23	26	7	8	16	15
7	12	108	104	2	27	48	45	11	1	24	26	4	2	65	67	5	1	52	53	7	10	24	27
7	13	30	24	2	28	50	52	11	2	26	25	4	3	85	85	5	2	50	50	7	11	30	29
7	15	63	60	3	1	28	29	11	3	31	29	4	4	150	152	5	3	56	59				
7	16	25	26	3	7	20	20	11	4	54	57	4	5	64	62	5	4	107	110				
7	18	54	50	3	9	24	27	11	5	24	21	4	6	90	48	5	5	42	43				
7	19	54	50	3	17	23	20	11	6	20	19	4	7	87	85	5	6	39	37				
7	20	67	66	4	3	21	19	11	7	32	30	4	8	24	30	5	7	60	60				
7	23	45	40	4	5	19	20	11	10	28	26	4	9	42	44	5	9	34	31				
7	26	31	34	5	0	31	31	11	11	33	30	4	10	69	70	5	10	52	57				
8	9	22	14	5	1	87	89					4	11	78	78	5	11	59	57				
10	0	22	21	5	2	74	74	***** K = 3 *****				4	12	113	115	5	12	88	87				
10	1	34	35	5	3	98	98					4	13	32	27	5	15	55	50				
10	2	33	35	5	4	175	172	3	0	305	308	4	14	28	27	5	18	39	42				
10	3	41	40	5	5	71	71	3	2	68	67	4	15	69	67	5	19	45	43				
10	4	76	77	5	6	55	52	3	4	58	58	4	18	55	55	5	20	55	57				
10	5	28	29	5	7	99	97	3	6	108	107	4	19	55	55	5	23	35	35				
10	6	25	26	5	8	37	31	3	8	242	255	4	20	69	72	8	1	34	30				
10	7	43	41	5	9	40	50	3	10	23	22	4	23	45	43	8	2	30	29				
10	9	22	22	5	10	77	77	3	12	27	29	4	24	19	21	8	3	36	36				
10	10	35	36	5	11	88	88	3	14	108	105	4	26	35	36	8	4	63	65				
10	11	40	40	5	12	122	128	3	16	156	158	4	27	35	34	8	5	25	25				
10	12	60	63	5	13	32	31	3	22	77	77	5	6	21	15	8	6	21	22				
10	15	37	36	5	14	32	29	3	24	83	84	7	1	45	43	8	7	36	35				
10	18	29	31	5	15	73	75	3	26	20	14	7	2	43	42	8	9	19	19				
				5	16	25	29	4	5	22	25	7	3	44	48	8	10	31	31				
***** K = 2 *****				5	18	56	60	5	1	23	24	7	4	90	92	8	11	36	34				
				5	19	59	60	6	0	179	183	7	5	37	35	8	12	53	54				
2	0	46	44	5	20	77	78	6	2	44	47	7	6	27	31	8	15	35	32				
2	1	142	148	5	23	52	47	6	4	28	27	7	7	51	49								
2	2	113	107	5	26	35	39	6	6	71	70	7	9	25	26	***** K = 6 *****							
2	3	154	162	5	27	37	36	6	8	164	159	7	10	43	43								
2	4	265	274	5	28	42	43	6	14	71	70	7	11	50	47	6	0	112	112				
2	5	113	115	8	1	44	47	6	16	116	109	7	12	69	73	6	2	26	30				
2	6	72	68	8	2	44	46	6	22	56	55	7	14	20	17	6	6	42	44				
2	7	151	156	8	3	55	53	6	24	62	62	7	15	46	42	6	8	98	100				
2	8	41	37	8	4	108	100	8	1	70	18	7	18	39	36	6	14	68	65				
2	9	78	78	8	5	37	39	8	9	20	19	7	19	38	36	6	16	76	73				
2	10	106	107	8	6	33	34	8	10	18	6	7	20	48	49								
2	11	133	135	8	7	52	54	9	0	103	103	9	13	17	13								

TABLE III

FINAL PARAMETERS FOR SEMICONDUCTING $Fe_{0.16}ZrSe_{1.94}$[a]

Atom	Wyckoff notation	Site symmetry	Occupancy	x	y	z	B (Å^2)
Zr	1*a*	$\bar{3}m$	1	0	0	0	0.46 (13)
Fe	1*b*	$\bar{3}m$	0.16 (3)	0	0	$\frac{1}{2}$	3.7 (11)
Se	2*d*	3*m*	0.97 (3)	$\frac{1}{3}$	$\frac{2}{3}$	0.7420 (3)[b]	0.83 (11)

[a] Secondary extinction coefficient = 0.27 (4) 10^{-5} e^{-2}.

[b] This parameter is 0.74, rather than the usual 0.26 in $ZrSe_2$, because of our choice of the opposite direction for the *c*-axis in the present determination. Figure 1 has been drawn for a z of 0.26.

motion and for secondary extinction along with a variable occupancy factor for the Fe atom placed in the 2*c* position. This cycle resulted in values of R and R_w of 0.051 and 0.067 and to a Fe/Zr ratio of 0.306 (5). Because the chemical analysis of the bulk sample led to Fe/Zr of 0.465 (15) and because the difference Fourier map (v.s.) showed peaks in the 2*b* and 2*d* as well as the 2*c* position an additional refinement was carried out in which Fe of variable occupancy was added to the 2*b* and 2*d* positions. Resulting values of R and R_w were 0.040 and 0.047 and the Fe/Zr ratio was 0.41 (3). However, the 2*d* site was only 10 (3)% occupied and the thermal parameter of the Fe atom in this site was comparatively high at 4.3 (27) Å^2. Refinement with this position unoccupied led to substantially unchanged agreement indices and Fe/Zr ratio owing to a high correlation between the occupancy factors of Fe in the 2*b* and 2*d* positions. Using this model, structure factor calculations for both possible enantiomers were made for the entire data set. The differences between Friedel pairs were less than experimental error owing to the nearly centric nature of the structure. In the final calculations the entire data set was used. Refinement of the "one-site" model with Fe in 2*c* led to values of R and R_w of 0.039 and 0.058 and an Fe/Zr ratio of 0.305 (4). Refinement of the "two-site" model with Fe in 2*b* and 2*c* led to values of 0.037 and 0.045 and an Fe/Zr ratio of 0.405 (12). Although the thermal parameter for Fe in site 2*b* was high at 2.5 Å^2, the two-site model has been retained, both because of the better agreement indices and because of the resulting Fe/Zr ratio that is closer to the chemical analysis. But it must be emphasized that the evidence for partial occupancy of 40% in the 2*b* position is not strong. Whether or not this position is truly occupied has no effect on the discussion below.

TABLE IV

INTERATOMIC DISTANCES IN SEMICONDUCTING $Fe_{0.16}ZrSe_{1.94}$

Atoms	Distances (Å)	Comments
Zr–Se	2.685 (1) (2.70 (2))[a]	
Zr–Fe	3.059 (1)	Along *c*-axis
Zr–Zr	3.763 (1) (3.770 (2))	In $z = 0$ plane
Fe–Se	2.629 (1)	
Fe–Fe	3.763 (1)	In $z = 0$ plane
Se–Se In plane $z = 0.74$	3.763 (3) (3.770 (2))	Edge shared by octahedra around Zr and Fe
Se–Se Through $z = 0$ plane	3.831 (3) (3.86 (5))	Octahedron around Zr
Se–Se Through $z = \frac{1}{2}$ plane	3.673 (3) (3.66 (3))	Octahedron around Fe

[a] Distances given in parentheses are the corresponding ones in the $ZrSe_2$ phase with the highest Se/Zr ratio at 800°C (*17*).

TABLE V

FINAL PARAMETERS FOR METALLIC $Fe_{0.41}ZrSe_2$[a]

Atom	Wyckoff notation	Symmetry	Occupancy	x	y	z	B (Å^2)
Zr(1)	$4f$	3	1	$\frac{1}{3}$	$\frac{2}{3}$	0.0010 (1)	0.22 (7)
Zr(2)	$2a$	32	1	0	0	0	0.26 (12)
Fe(1)	$2c$	32	0.79 (1)	$\frac{1}{3}$	$\frac{2}{3}$	$\frac{1}{4}$	0.32 (5)
Fe(2)	$2b$	32	0.40 (2)	0	0	$\frac{1}{4}$	2.5 (6)
Se	$12i$	1	1	0.6732 (6)	0.0060 (2)	0.1302 (1)	0.496 (18)

[a] Secondary extinction coefficient = 0.103 (4) 10^{-4} e^{-2}.

Analysis of $\sum w(|F_o| - |F_c|)^2$ as a function of $|F_o|$, setting angles, and Miller indices revealed no unusual trends. The error in an observation of unit weight is 1.4 electrons for this refinement of 13 variables based on 574 observations. Of the 1207 reflections omitted from the refinement because $F_o^2 < 3\sigma(F_o^2)$ only 5 had $|F_o^2 - F_c^2| > 3\sigma(F_o^2)$. On a final difference Fourier map the maximum electron density is 7 e/A^3, less than 1 % of the height of a Zr atom on a Fourier map.

Observed and calculated structure amplitudes are listed in Table IIb. Atomic parameters are given in Table V and selected distances are given in Table VI.

TABLE VI

INTERATOMIC DISTANCES IN METALLIC $Fe_{0.41}ZrSe_2$

Atoms	Distances (Å)	Comments
Zr(1)–Se	2.601 (2)	
	2.627 (2)	
Zr(1)–Fe(1)	3.184 (1)	Along c-axis
Zr(1)–Zr(1)	3.471 (1)	In $z \approx 0$ plane
Zr(1)–Zr(2)	3.470 (1)	
Zr(2)–Se	2.589 (3)	
Zr(2)–Fe(2)	3.197 (1)	Along threefold axis in $z \approx 0$ plane
Fe(1)–Fe(2)	3.470 (1)	
Fe(1)–Se	2.552 (2)	
Fe(2)–Se	2.505 (3)	
Se–Se In $z \approx \frac{1}{8}$ plane	3.434 (7)	Edges shared by octahedron and trigonal prisms
	3.442 (4)	
	3.536 (3)	
Se–Se Through $z = \frac{1}{4}$ plane	3.678 (3)	Octahedra around Fe
	3.683 (4)	
	3.619 (3)	
Se–Se Through $z = 0$ plane	3.331 (1)	Trigonal prisms around Zr

Discussion

The structure of $Fe_{0.16}ZrSe_{1.94}$ can be derived from that of $ZrSe_2$ by inserting the Fe atoms in octahedral interstices between the layers; the structure may be regarded as the usual CdI_2–NiAs type (Fig. 1). In the resulting structure the Fe atoms occupy octahedral holes instead of tetrahedral holes as was found by Trichet and Rouxel (*1*, *2*) in the system M_xZrS_2 (M = Fe, Co, Ni).

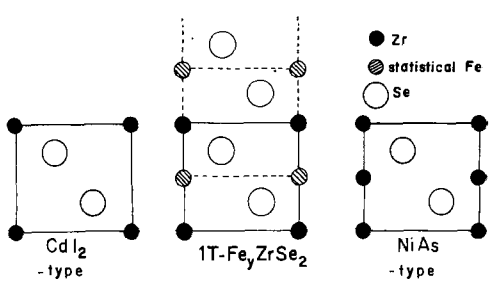

FIG. 1. Views in the (110) plane of semiconducting Fe_yZrSe_2 and of CdI_2 and NiAs type structures.

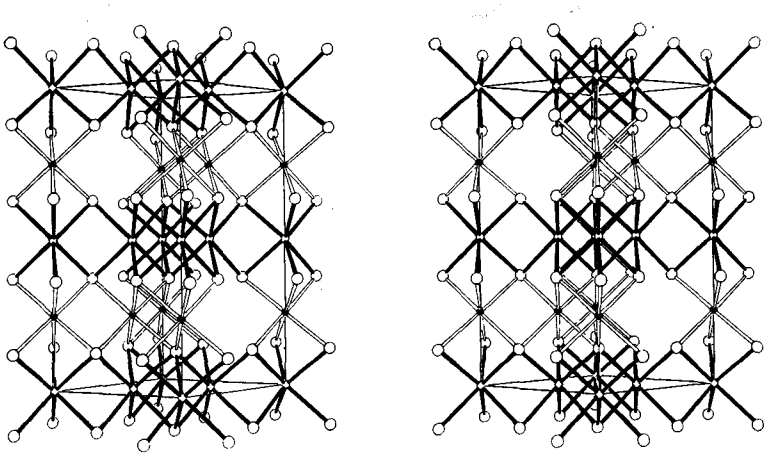

FIG. 2. Stereo view of the structure of metallic $Fe_{0.41}ZrSe_2$. Se are large open circles; Zr are small open circles; Fe are dark circles.

The Se octahedra are not exactly regular. Interatomic distances (Table IV) for edges through the $z = 0$ plane, that is, around a Zr atom, are larger than edges perpendicular to the threefold axis: 3.831 (3) and 3.763 (1) Å, respectively. The opposite occurs around an Fe atom since edges through the $z = \frac{1}{2}$ plane are 3.673 (3) Å. The Se–Se and Se–Zr distances do not differ significantly from those in $ZrSe_2$ (Table IV).

The structure of $Fe_{0.41}ZrSe_2$ shown in Fig. 2 is the same as the one previously described by Anzenhofer, van den Berg, Cossee, and Helle for the compounds $M Nb_3S_6$ (M = Mn, Fe, Co, Ni) (*21*). As shown in Fig. 3, it is a superstructure of the 2H–$Nb_{1+x}S_2$ type

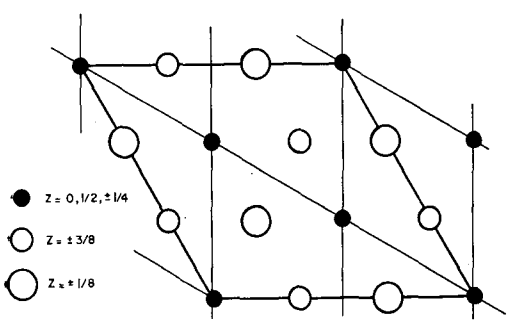

FIG. 3. Projection on (001) plane showing structural relation between 2H–$Nb_{1+x}S_2$ type structure (thin lines) and the structure of 2H–$Fe_{0.41}ZrSe_2$. Metallic atoms are dark circles and nonmetallic atoms are open circles.

(*22*): The hexagonal array of $Fe_{0.41}ZrSe_2$ is built on the [110] face diagonal of 2H–$Nb_{1+x}S_2$ lattice type. The structure thus obtained consists of alternate layers of Se octahedra and Se trigonal prisms stacked along the z-axis. The sequence of single Se sheets is ---*A B B A*---, with x and y coordinates being about $(\frac{2}{3}, 0; 0, \frac{2}{3}; \frac{1}{3}, \frac{1}{3})$ for A and $(\frac{1}{3}, 0; 0, \frac{1}{3}; \frac{2}{3}, \frac{2}{3})$ for B.

As a consequence, the Se atoms about the Zr impart a trigonal prismatic environment to the Zr atom. Hence, this structure cannot be related to that of $ZrSe_2$, in which Zr atoms are located in half the available octahedral holes (CdI_2 type). Insofar as we know this is the first time a chalcogenic trigonal prismatic coordination has been clearly established for a group IVB metal in an inorganic solid state compound.[2]

The octahedral holes are either vacant or are occupied by Fe atoms, giving rise to a partial ordering. From the occupancy factors of Fe, it follows that $\frac{2}{3}$ of the Fe atoms are randomly distributed in 2*c* sites, while the remaining $\frac{1}{3}$ are randomly distributed in 2*b* sites. The pattern of metal atoms (both Zr and statistical Fe) in the (110) plane is the same as

[2] As reported by Flahaut (*23*), the *WC* type of structure, which implies trigonal prismatic coordination of metal atoms, has been suggested for the subchalcogenides ZrS_{1-x}, $ZrSe_{1-x}$, and HfS_{1-x}, but its existence has not been absolutely demonstrated.

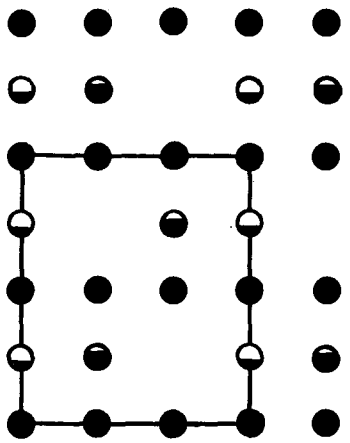

FIG. 4. View in the (110) plane of metallic $Fe_{0.41}ZrSe_2$ showing the partial ordering of Fe atoms (black and white circles). Zr atoms are black circles.

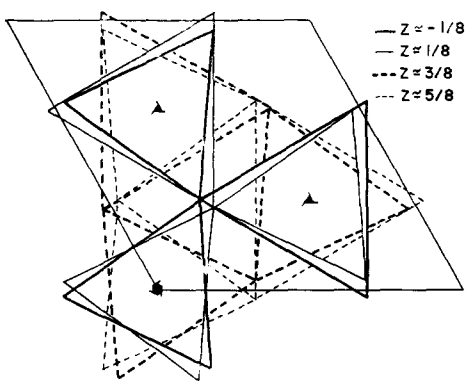

FIG. 5. Metallic $Fe_{0.41}ZrSe_2$ projection on the (001) plane. The distortion of octahedra and trigonal prisms around the metal atoms have been exaggerated for the sake of clarity.

that of the Cr atoms in Cr_5S_6, described by Jellinek (*24*) as having a supercell ($a' = a\sqrt{3}$; $c' = 2c$) derived from the NiAs–CdI_2 intermediate type (Fig. 4).

The Se trigonal prisms and octahedra are not exactly regular. Successive faces of a trigonal prism should be eclipsed, while those of an octahedron should be twisted by 60°. The twist angles (1.82, 0.91, 61.82, 58.18, 61.97, and 60.15°) deviate slightly from the ideal values. These deviations are illustrated in Fig. 5. It also can be seen that the trigonal prisms around Zr atoms on the threefold axis have triangular faces of different dimensions: 3.442 (6) Å and 3.536 (3) Å. On the other hand, both the top and bottom faces of the octahedra have the same edge dimension, but this dimension is 3.536 (3) Å along the $(\frac{1}{3}, \frac{2}{3})$ axis, 3.442 (4) Å along the $(\frac{2}{3}, \frac{1}{3})$ axis and alternately 3.434 (7) and 3.442 (6) Å along the sixfold axis. Finally, the distance between two successive Se sheets is alternately 3.063 Å (octahedron height) and 3.331 Å (trigonal prism height).

The Se–Se distances range from 3.331 (1) to 3.683 (4) Å while in $ZrSe_2$ they range from 3.679 to 3.839 Å. The van der Waals' radius of Se is 1.96 Å (*25*). The Zr–Se distances range from 2.589 (3) to 2.627 (2) Å, and on the average are about 0.10 Å shorter than in $ZrSe_2$ (2.691 Å (*16*)). The Fe–Se distances of 2.552 (2) and 2.505 (3) Å are shorter than in the semiconducting $Fe_{0.16}ZrSe_2$ phase (2.629 (1) Å). Note that the Zr–Zr, Fe–Fe, and Fe–Zr distances (Table VI) are significantly greater than is calculated from elemental radii (1.60 Å for Zr and 1.26 Å for Fe (*26*)). Thus, the observed metallic behavior cannot be explained by a simple metal–metal bonding arrangement.

The changes in electrical properties and Zr coordination in these two phases suggest that Zr has undergone a change in electronic configuration from d^0, characteristic of group IVB dichalcogenides, to a "group VB-like" d^1 configuration. This is consistent with Gamble's (*5*) point of view that structure is closely related to electronic configuration in these types of compounds. In fact, band calculations have shown that the trigonal prismatic coordination is more stable for metal atoms with a d^1 configuration (e.g., 2H–$TaSe_2$, 2H–$NbSe_2$, and their derivatives; *5*, *27*).

Acknowledgments

We wish to thank Dr. M. T. Ratajack for electrical conductivity measurements. This work was supported in part by the National Science Foundation through the Northwestern University Materials Research Center. The first author wishes to thank the North Atlantic Treaty Organization for a Fellowship.

References

1. L. TRICHET AND J. ROUXEL, *C. R. Acad. Sci.* **267**, 1322 (1968); **269**, 1040 (1969).
2. L. TRICHET, Thèse de Doctorat-ès-Sciences, Université de Nantes, France (1973).
3. L. TRICHET, J. COUSSEAU, AND J. ROUXEL, *C. R. Acad. Sci.* **273**, 243 (1971).
4. J. COUSSEAU, Thèse de Doctorat de Spècialitè, Université de Nantes, France (1973).
5. F. R. GAMBLE, *J. Solid State Chem.* **9**, 358 (1974).
6. M. M. VAN DEN BERG AND P. COSSEE, *Inorg. Chim. Acta* **2**, 143 (1968).
7. J. M. VAN DEN BERG AND M. ROBBIN, *J. Solid State Chem.* **1**, 134 (1970).
8. A. MEERSHAUT AND J. ROUXEL, *C. R. Acad. Sci.* **277**, 163 (1973).
9. A. E. VAN ARKEL, *Physica* **4**, 286 (1924).
10. K. F. MCTAGGART, *Aust. J. Chem.* **11**, 445 (1958).
11. D. L. GREENAWAY AND R. NITSCHE, *J. Phys. Chem. Solids* **26**, 1445 (1965).
12. A. AHOUANDJINOU AND L. TRICHET, to appear.
13. J. F. REVELLI, M. T. RATAJACK, A. GLEIZES, L. SCHWARTZ, J. B. WAGNER, AND C. R. KANNEWURF, *Bull. Amer. Phys. Soc.* **20**, 487 (1975).
14. H. SCHAEFER, "Chemical Transport Reactions," Academic Press, New York (1964).
15. R. J. DOEDENS AND J. A. IBERS, *Inorg. Chem.* **6**, 204 (1967).
16. A. GLEIZES AND Y. JEANNIN, *J. Solid State Chem.* **1**, 180 (1970).
17. A. GLEIZES, Thèse de Doctorat-ès-Sciences, Universitè Paul Sabatier, Toulouse, France (1974).
18. In addition to various local programs for the CDC 6400 computer, modified versions of the following programs were employed: Zalkin's FORDAP Fourier summation program, Johnson's ORTEP thermal ellipsoid plotting program, Busing and Levy's ORFFE error function program. Our full-matrix least-squares program, NUCLS, in its nongroup form closely resembles the Busing–Levy ORFLS program. The Northwestern absorption program, AGNOST, includes both Gaussian integration and analytical methods. Absorption corrections carried out for the present compounds were via the analytical method.
19. J. A. IBERS, *Acta Crystallogr.* **22**, 604 (1967).
20. D. T. CROMER AND J. T. WABER, "International Tables for X-ray Crystallography," Vol. IV, Table 2.2A, Kynoch Press, Birmingham, England (1974); D. T. CROMER, *ibid.*, Table 2.3.1.
21. K. ANZENHOFER, J. M. VAN DEN BERG, P. COSSEE, AND J. N. HELLE, *J. Phys. Chem. Solids* **31**, 1057 (1970).
22. F. JELLINEK, *J. Less Common Met.* **4**, 9 (1962).
23. J. FLAHAUT, "Transition Metal Chalcogenides," Med. Tech. Publ. Co. (1972); *Int. Rev. Sci.: Inorg. Chem., Ser. 1* **10**, 189 (1972).
24. F. JELLINEK, *Acta Crystallogr.* **10**, 620 (1957).
25. L. PAULING, "The Nature of the Chemical Bond," Cornell University Press, Ithaca, N.Y. (1964).
26. J. P. JESSON AND E. L. MUETTERTIES "Chemist's Guide. Basic Chemical and Physical Data," Dekker, New York (1969).
27. R. HUISMAN, R. DEJONGE, C. HAAS, AND F. JELLINEK, *J. Solid State Chem.* **3**, 56 (1971).